arXiv:cond-mat/0310039v2 18 Nov 2003

Spin relaxation in semiconductor quantum dots

J. L. Cheng,[1,2] M. W. Wu,[1,2,*] and C. Lü[2]
[1]*Structure Research Laboratory, University of Science &Technology of China, Academia Sinica, Hefei, Anhui, 230026, China*
[2]*Department of Physics, University of Science &Technology of China, Hefei, Anhui, 230026, China*[†]

(Dated: February 2, 2008)

The spin relaxation time due to the electron-acoustic phonon scattering in GaAs quantum dots is studied after the exact diagonalization of the electron Hamiltonian with the spin-orbit coupling. Different effects such as the magnetic field, the quantum dot size and the temperature on the spin relaxation time are investigated in detail. Moreover, we show that the perturbation method widely used in the literature is inadequate in accounting for the electron structure and therefore the spin relaxation time.

PACS numbers: 71.70.Ej, 73.21.La,72.25.Rb

I. INTRODUCTION

Spin-related phenomena in semiconductors have attracted much attention recently as they are the key ingredient in the field of spintronics.[1] Among these, the spin-orbit coupling mechanisms in semiconductor quantum dots (QDs) provide a basis for device applications such as qubits in quantum computers and have therefore caused much interest.[2,3,4,5,6,7] Voskoboynikov *et al.* studied the electron structures of QDs by exactly diagonalizing the Hamiltonian with spin-orbit coupling.[8] Governale studied the electron structure of few-electron interacting QDs with Rashba spin-orbit coupling by spin density functional theory.[9] Valín-Rodríguez *et al.* investigated spin procession in QDs with the spin-orbit coupling.[2] Besides the effect of the spin-mixing in the electron structure, the spin-orbit coupling also induces the spin relaxation via further coupling with phonons, which alone conserve the spin and therefore are unable to cause any spin relaxation. Many works calculated the spin relaxation time (SRT) due to the spin-orbit coupling induced spin-flip electron-phonon scattering at zero or very low temperatures.[4,6,7,10] Unlike the electron structure calculation,[2,8,9] to our knowledge all works on the SRT are based on perturbation theory where the spin-orbit coupling is treated as a perturbation in the Hilbert space spanned by H_0 which does not include the spin-orbit coupling. Moreover only the lowest few energy levels of H_0 are included in the theory.[4,6,7,10] Whether the perturbation based on the lowest few levels of H_0 is adequate remains unchecked.

In the present paper, we investigate the SRT of GaAs QDs confined in the quantum well by parabolic potentials by exactly diagonalizing the total Hamiltonian. We calculate the SRT due to the scattering with the acoustic phonons by the Fermi golden rule after getting the energy spectra and the wavefunctions from the exact diagonalization. We find that the perturbation approach is inadequate in calculating the SRT and therefore it is necessary to reinvestigate the accurate SRT via the exact diagonalization approach. We organize the paper as follows: In Sec. II we set up our model and the Hamiltonian. Then in Sec. III we present our numerical results: We first compare the results obtained from our exact diagonalization method with those from the perturbation approach and show that the perturbation method is inadequate in accounting for the SRT in Sec. III(A). In Sec. III(B) we discuss the SRT of a small QD at $T = 4$ K where only the lowest two energy levels of the total electron Hamiltonian after the exact diagonalization account for the SRT. Nevertheless at least 12 energy levels of H_0 are needed to get these lowest two energy levels. We then turn to effects of the magnetic field, the temperature and the quantum well width to the SRT in Sec. III(C)-(E). We give our conclusions in Sec. IV.

II. MODEL AND HAMILTONIAN

We set up a simplified model to study the spin relaxation in the QD's which are defined by parabolic potentials $V_c(\mathbf{r}) = \frac{1}{2}m^*\omega_0^2\mathbf{r}^2$ in a quantum well of width a. A magnetic field $\mathbf{B}$ is applied along the growth (z) direction of the quantum well. The total Hamiltonian is given by

$$H = H_e + H_{ph} + H_{ep} \tag{1}$$

with the electron Hamiltonian $H_e = H_0 + H_{so}$. Here H_0 is electron Hamiltonian without the spin-orbit coupling:

$$H_0 = \frac{\mathbf{P}^2}{2m^*} + V_c(\mathbf{r}) + H_B \tag{2}$$

in which $\mathbf{P} = -i\hbar\boldsymbol{\nabla} + (e/c)\mathbf{A}$ with $\mathbf{A} = \frac{B}{2}(-y, x, 0)$ stands for the electron momentum operator. m^* is the electron effective mass. $H_B = \frac{1}{2}g\mu_B B\sigma_z$ is the Zeeman energy with $\boldsymbol{\sigma}$representing the Pauli matrices. $H_{so} = \gamma\mathbf{h}\cdot\boldsymbol{\sigma}$ is the spin-orbit coupling which is the key to the spin flip and spin relaxation. $\mathbf{h} = [P_x(P_y^2 - P_z^2), P_y(P_z^2 - P_x^2), P_z(P_x^2 - P_y^2)]$ is the Dresshauls effective magnetic field in the bulk material.[11] In quantum well with small width, H_{so} can be simplified as

$$H_{so} = \gamma_c(-P_x\sigma_x + P_y\sigma_y) \tag{3}$$

with $\gamma_c = \gamma(\pi/a)^2$. H_{ph} in Eq. (1) is the Hamiltonian for phonons and is given by $H_{ph} = \sum_{\mathbf{q}\lambda} \hbar\omega_{\mathbf{q}\lambda} a^\dagger_{\mathbf{q}\lambda} a_{\mathbf{q}\lambda}$ with $\omega_{\mathbf{q}\lambda}$ standing for the phonon energy spectrum of branch λ and momentum $\mathbf{q}$. The electron-phonon scattering is given by

$$H_{ep} = \sum_{\mathbf{q}\lambda} M_{\mathbf{q}\lambda}(a^\dagger_{\mathbf{q}\lambda} + a_{\mathbf{q}\lambda}) \exp(i\mathbf{q}\cdot\mathbf{r}) \qquad (4)$$

with $M_{\mathbf{q}\lambda}$ being the scattering matrix element.

We diagonalize the electron Hamiltonian H_e in the Hilbert space $|n,l,\sigma\rangle$ constructed by $H_0 = \frac{\mathbf{P}^2}{2m^*} + V_c(\mathbf{r}) + H_B$: $|\Psi_\ell\rangle = \sum_{nl\sigma} C^\ell_{nl\sigma}|n,l,\sigma\rangle$. Here $H_0|n,l,\sigma\rangle = E_{n,l,\sigma}|n,l,\sigma\rangle$ with

$$\langle\mathbf{r}|n,l,\sigma\rangle = N_{n,l}(\alpha r)^{|l|} e^{-\frac{(\alpha r)^2}{2}} L_n^{|l|}((\alpha r)^2) e^{il\theta}\chi_\sigma \ , \qquad (5)$$

and

$$E_{n,l,\sigma} = \hbar\Omega(2n + |l| + 1) - \hbar\omega_B l + \sigma E_B \ . \qquad (6)$$

In these equations $n = 0, 1, 2, \cdots$ and $l = 0, \pm1, \pm2, \cdots$ are quantum numbers. $\Omega = \sqrt{\omega_0^2 + \omega_B^2}$ and $\omega_B = eB/(2m^*)$. $N_{n,l} = \left(\frac{\alpha^2 n!}{\pi(n+|l|)!}\right)^{\frac{1}{2}}$ with $\alpha = \sqrt{m^*\Omega/\hbar}$. $E_B = \frac{1}{2}g\mu_B B$ is the Zeeman splitting energy. $\sigma = \pm1$ refers to the spin polarization along the z-axis. χ_σ represents the eigenfunction of σ_z. $L_n^{|l|}$ is the generalized Laguerre polynomial. By solving

$$H_e|\Psi_\ell\rangle = \epsilon_\ell|\Psi_\ell\rangle \ , \qquad (7)$$

one can determine the eigenenergy ϵ_ℓ and the eigenfunction of the total electron system H_e. It is noted that due to the presence of the spin-orbit coupling H_{so}, σ is no longer a good quantum number. Mixing occurs for opposite spins:

$$\langle n,l,\sigma|H_{so}|n',l',\sigma'\rangle = i2\pi\gamma_c\alpha\delta_{l'+\sigma,l}\delta_{\sigma,-\sigma'}[\sigma(\omega_B/\Omega)A^{(1)}_{n,n',l,l'} - \sigma l' A^{(2)}_{n,n',l,l'} + A^{(3)}_{n,n',l,l'}] \ . \qquad (8)$$

It is this mixing that makes the originally spin-conserving electron-phonon scattering Eq. (4) cause spin relaxation.

$A^{(1)}$ to $A^{(3)}$ in Eq. (8) are given in detail in Appendix A.

The eigenfunction $|\Psi_\ell\rangle$ obtained from Eq. (7) contains spin mixing for each state ℓ. We assign an eigen state ℓ to be spin-up if $\bar{\sigma}_z = \langle\Psi_\ell|\sigma_z|\Psi_\ell\rangle > 0$ or spin-down if $\bar{\sigma}_z < 0$. An electron at initial electron state i with energy ϵ_i and a spin polarization can be scattered by the phonon into another state f with energy ϵ_f and the *opposite* spin polarization. The rate of such scattering can be described by the Fermi golden rule:

$$\begin{aligned}\Gamma_{i\to f} &= \frac{2\pi}{\hbar}\sum_{\mathbf{q}\lambda}|M_{\mathbf{q}\lambda}|^2|\langle f|e^{i\mathbf{q}\cdot\mathbf{r}}|i\rangle|^2[\bar{n}_{\mathbf{q}\lambda}\delta(\epsilon_f - \epsilon_i - \omega_{\mathbf{q}\lambda}) \\ &\quad + (\bar{n}_{\mathbf{q}\lambda}+1)\delta(\epsilon_f - \epsilon_i + \omega_{\mathbf{q}\lambda})] \ , \qquad (9)\end{aligned}$$

with $\bar{n}_{\mathbf{q}\lambda}$ representing the Bose distribution of phonon with mode λ and momentum q at the temperature T. Its expression after the integration is given in Appendix B. The SRT τ can therefore be determined by

$$\frac{1}{\tau} = \sum_i f_i \sum_f \Gamma_{i\to f} \ , \qquad (10)$$

in which $f_i = C\exp[-\epsilon_i/(k_B T)]$ denotes the Maxwell distribution of the i-th level with C being a constant.

III. NUMERICAL RESULTS

We perform a numerical investigation of the SRT [Eq. (10)] in GaAs quantum dots at low temperatures by diagonalizing the Hamiltonian H_e for each given dot size: the quantum well width a and the effective diameter $d = \sqrt{\frac{\hbar\pi}{m^*\omega_0}}$, as well as each given applied magnetic field B. To do so, we gradually increase the number of basis function arranged in the order of energy in the Hilbert space $|n,l,\sigma\rangle$ to ensure the 0.1 % precision of the converged energy ϵ_ℓ. As an example for a QD with $B = 1$ T and $a = 5$ nm, when $d = 20$ nm, in order to converge the lowest 2 (100) levels, one has to use 12 (120) basis functions; nevertheless, when $d = 60$ nm, in order to converge the lowest 2 (100) levels, one has to use 20 (200) basis functions.

D	5.3×10^3kg/m^3	κ	12.9
v_{st}	2.48×10^3 m/s	g	-0.44
v_{sl}	5.29×10^3 m/s	Ξ	7.0 eV
e_{14}	1.41×10^3 V/m	m^*	$0.067m_0$

TABLE I: Parameters used in the calculation

The electron-phonon scattering is composed of the following contributions: (i) The electron-acoustic phonon scattering due to the deformation potential with $M^2_{\mathbf{q}sl} = \frac{\Xi^2 q}{2Dv_{sl}}$; (ii) The electron-acoustic phonon scattering due to the piezoelectric field for the longitudinal phonon mode with $M^2_{\mathbf{q}pl} = \frac{32\pi^2 e^2 e^2_{14}}{\kappa^2 D v_{sl}}\frac{(3q_x q_y q_z)^2}{q^7}$ and for the two transverse phonon modes with $\sum_{j=1,2} M^2_{\mathbf{q}pt_j} =$

$\frac{32\pi^2 e^2 e_{14}^2}{\kappa^2 D v_{st} q^5}[q_x^2 q_y^2 + q_y^2 q_z^2 + q_z^2 q_x^2 - \frac{(3q_x q_y q_z)^2}{q^2}]$. Here Ξ stands for the acoustic deformation potential, D is the GaAs volume density, e_{14} represents the piezoelectric constant and κ denotes the static dielectric constant. The acoustic phonon spectra $\omega_{\mathbf{q}\lambda}$ are given by $\omega_{\mathbf{q}l} = v_{sl} q$ for the longitudinal mode and $\omega_{\mathbf{q}pt} = v_{st} q$ for the transverse mode with v_{sl} and v_{st} representing the corresponding sound velocities. It is noted that notwithstanding the fact that we include all these acoustic phonons throughout our computation, for all the cases we have studied in this paper, the main contribution comes from the electron-phonon scattering due to the piezoelectric field for the transverse mode with the later being at least one order of magnitude larger than the other phonon modes. Moreover, the contribution from LO-phonon is negligible in the temperature regime we are studying. The parameters used in our calculation are listed in Table I.[13]

A. Comparison with previous works at $T = 4$ K

We first compare our approach with the perturbation calculations widely used in the literature[6,7,10] at low temperature to double check the validity of our method as well as that of the perturbation method where H_{so} is treated as the perturbation. Following the previous works,[6,7,10] we calculate the SRT between the lowest two Zeeman splitting levels at $d = 20$ nm and $T = 4$ K. Unless specified, the width of the quantum well a is fixed to be 5 nm throughout the paper. To the first order of H_{so}, the energy difference of the lowest two states with the opposite spins is $\Delta E = 2E_B$ (the first order correction is zero) and the wave functions of these two states are

$$\begin{aligned} \Psi_\uparrow &= \langle r|0,0,\uparrow\rangle , \\ \Psi_\downarrow &= \langle r|0,0,\downarrow\rangle - \mathcal{A}\langle r|0,1,\uparrow\rangle , \end{aligned} \tag{11}$$

in which $\mathcal{A} = i\hbar\gamma_c(\frac{\pi}{a})^2 \frac{\alpha(1-eB/(2\hbar\alpha^2))}{E_{0,1,\uparrow} - E_{0,0,\downarrow}}$. The SRT τ is therefore given by

$$\begin{aligned} \frac{1}{\tau} &= c|\mathcal{A}|^2 \bar{n}_q q^3 \int_0^{\frac{\pi}{2}} d\theta \sin^5\theta (\sin^4\theta + 8\cos^4\theta) \\ &\quad \times \exp(-\frac{1}{2}q^2 \sin^2\theta) I^2(q\cos\theta) , \end{aligned} \tag{12}$$

with $q = \Delta E/(\hbar v_{st}\alpha)$, $c = 9\pi\alpha e^2 e_{14}^2/(\hbar D v_{st}^2 \kappa^2)$ and $I(q_z) = 8\pi^2 \sin(aq_z/2)/\{aq_z[4\pi^2 - (aq_z)^2]\}$. This is exactly the same calculation used in the literature.[6,7,10]

In Fig. 1 we compare the SRT calculated from Eq. (12) (curve with ■) with our exact diagonalization method (curve with ◯) described in the previous section, but with only the lowest four levels of the Hilbert space, *ie.*, $|0,0,\sigma\rangle$ and $|0,1,\sigma\rangle$ ($\sigma =\uparrow$ or $\downarrow$), taken, corresponding to the same levels used in the perturbation method. It is seen from the figure that there is at least one order of magnitude difference between the two curves: τ obtained from the perturbation method is much larger than the one from the exact diagonalization method. Moreover, the trends of the magnetic field dependence are also different. We point out that these differences arise from the fact that only the first order of the perturbation is applied. It can be fixed if one further includes the second order correction in ΔE, *ie.* $\Delta E = 2E_B + |\mathcal{A}|^2(E_{0,1,\uparrow} - E_{0,0,\downarrow})$. It is noted that the second order correction to the energy difference is much larger than $2E_B$, the unperturbed energy difference. The SRT calculated from the perturbation method, modified with the energy correction to the second order, is plotted as a function of the magnetic field B in the same figure (curve with ×). One notices that it exactly hits on the curve from our diagonalization method (curve with ◯).

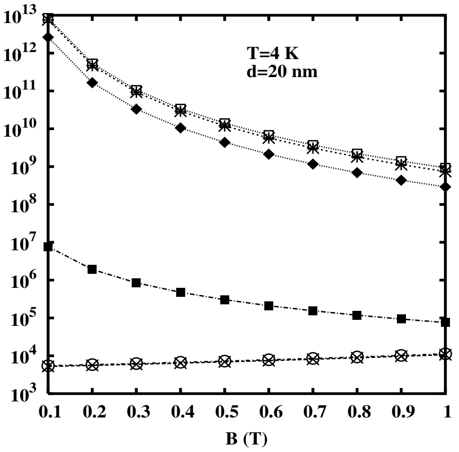

FIG. 1: SRT versus the magnetic field. Curve with ■: perturbation result without energy corrections; Curve with ◯: diagonalization result but with only the lowest four levels used as basis functions; Curve with ×: Perturbation result with the second order energy correction;Curve with ◆: exact diagonalization result with the energy sufficiently converged; Curve with □: diagonalization result with the lowest six levels used as basis functions; Curve with ✱: perturbation result with the lowest six levels of H_0 as basis functions and with the second order energy correction.

We notice that the diagonalization above includes only the lowest four levels. If it is adequate in converging the lowest two levels remains unchecked. As mentioned in the beginning of this section, that for the size of the dot we are studying here, in order to converge the lowest two energy levels, one has to use 12 basis functions. τ calculated from the exact diagonalization method is plotted in also Fig. 1 against the magnetic field (curve with ◆). Strikingly, it is *orders of magnitude* larger than that from the perturbation.

In order to understand this huge difference, now we include *six* lowest energy levels of H_0, *i.e.*, $|0,0,\uparrow\rangle$, $|0,0,\downarrow\rangle$, $|0,1,\uparrow\rangle$, $|0,1,\downarrow\rangle$, $|0,-1,\uparrow\rangle$ and $|0,-1,\downarrow\rangle$, as basis functions in the perturbation method. The wavefunctions of the lowest two states of H_e are therefore given by

$$\begin{aligned} \Psi_\uparrow &= \langle r|0,0,\uparrow\rangle - \mathcal{B}\langle r|0,-1,\downarrow\rangle , \\ \Psi_\downarrow &= \langle r|0,0,\downarrow\rangle - \mathcal{A}\langle r|0,1,\uparrow\rangle , \end{aligned} \tag{13}$$

in which

$$\mathcal{B} = i\hbar\alpha\gamma_c(\frac{\pi}{a})^2 \frac{1+eB/(2\hbar\alpha^2)}{E_{0,-1,\uparrow}-E_{0,0,\downarrow}} \ . \tag{14}$$

The energy difference between $\Psi_\uparrow$ and $\Psi_\downarrow$ now becomes

$$\Delta E = 2E_B + |\mathcal{A}|^2(E_{0,1,\uparrow}-E_{0,0,\downarrow}) - |\mathcal{B}|^2(E_{0,-1,\uparrow}-E_{0,0,\uparrow}) \ . \tag{15}$$

The corresponding SRT τ is hence given by

$$\begin{aligned}\frac{1}{\tau} &= c|\mathcal{A}-\mathcal{B}|^2\bar{n}_q q^3 \int_0^{\frac{\pi}{2}} d\theta \sin^5\theta(\sin^4\theta + 8\cos^4\theta) \\ &\quad \times \exp(-\frac{1}{2}q^2\sin^2\theta)I^2(q\cos\theta) \ , \end{aligned} \tag{16}$$

The numerical results of Eq. (16) are plotted by the curve with ✱ in Fig. 1. It is seen from the figure that the inclusion of the additional basis functions in the perturbation method also greatly enhances the SRT by orders of magnitude. The results obtained from the exact diagonalization method with the same lowest six levels as basis are given by the curve with □. The two curves are almost the same, and much closer to the final converged results (curve marked with ♦).

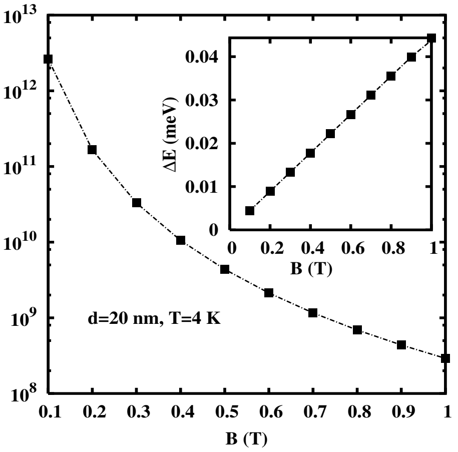

FIG. 2: SRT versus the applied magnetic field at d=20 nm and T=4 K. The inset is the corresponding energy splitting ΔE between the lowest two levels

It is clearly seen from the above calculation that the perturbation approach widely used in the literature is *inadequate* in describing the SRT even with the second order energy corrections included. In principal in order to use the perturbation method to calculate the SRT, one has to include sufficient number of the states in the basis in stead of only the lowest four levels widely used in the literature. This is of course inapplicable especially for larger QD's or higher temperature where one has to include a lot of basis functions (for a QD of $d = 60$ nm, one has to use 100 levels as basis functions) and the SRT is determined by many levels (in stead of only the lowest two) of the total electron Hamiltonian H_e. Even for the lowest two levels (for a QD with $d = 20$ nm at 4 K, the SRT is determined by the lowest two levels of the total electron Hamiltonian H_e), one has to use a lot of basis functions to converge the energy and the resulting SRT between these two levels is therefore strongly readjusted. This is because the spin-orbit coupling is very strong in mixing different energy levels of H_0.

In the following subsections, we therefore reinvestigate the properties of the SRT based on the exact diagonalization calculation.

B. SRT of a $d = 20$ nm QD at $T = 4$ K

As pointed out in the previous subsection that for a QD with $d = 20$ nm, at $T = 4$ K the SRT is determined by the spin-flip transition between the lowest two energy levels after the *exact diagonalization*, although at least 12 energy levels in the Hilbert space of H_0 are essential in getting these two levels. In this subsection we focus on the effects of the external fields on the SRT determined by these two levels.

It is seen from Eqs. (12) and (16) that in a given basis the spin relaxation rate $1/\tau$ is determined by two competing trends as a function of the energy splitting ΔE: (i) $q^3\bar{n}_q$, which increases with ΔE in the present case, and (ii) $\exp(-\frac{1}{2}q^2\sin^2\theta)I^2(q\cos\theta)$, which decreases with ΔE. Therefore, the SRT can be uniquely determined by the energy ΔE. For small ΔE, it is easy to see that the trend (i) dominates the when $\Delta E \lesssim 7.0\hbar v_{st}/d$, which is 0.57 meV at $d = 20$ nm. That is, the SRT decreases with ΔE when $\Delta E \lesssim 0.57$ meV.

In Fig. 2 the SRT is plotted against the applied magnetic field B. It is seen from the figure that τ decreases with the applied magnetic field. This is understood from the fact that the energy splitting ΔE increases with the applied magnetic field as shown in the inset. Moreover, even for the largest energy splitting 0.04 meV at $B = 1$ T, it is one order of magnitude smaller than 0.57 meV, energy splitting required to have the opposite τ-B dependence.

C. Magnetic field dependence of the SRT

We investigate the magnetic field dependence of the SRT for different diameters of the QD's at two different temperatures as shown in Fig. 3. Unlike the previous subsection where only the lowest two energy levels are important, here for most cases one has to include many levels of the total electron Hamiltonian.

It is seen that the SRT decreases rapidly with the magnetic field at each dot size and temperature. This feature is quite opposite to the bulk,[14] the two-[15] and the one-dimensional[16] cases where the SRT always increases with the magnetic field. This is because in the dot case there are only discrete energy levels and the magnetic field helps to increase the spin-flip scattering as discussed in

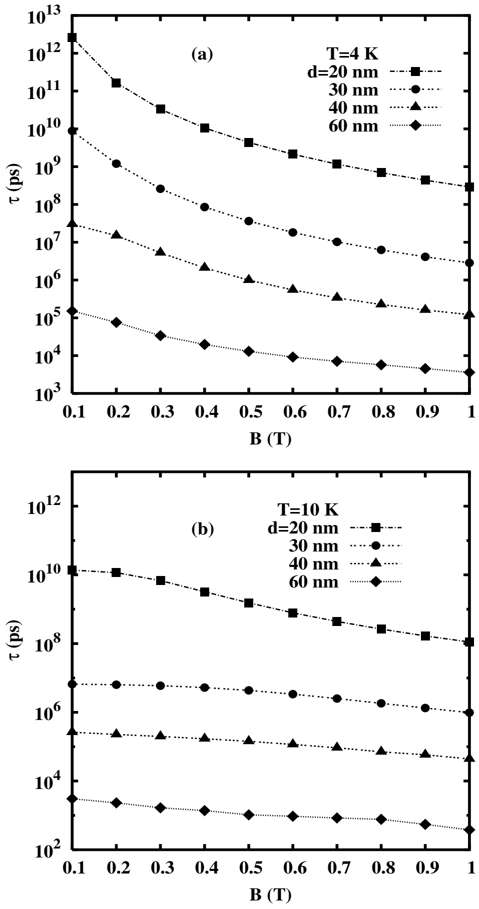

FIG. 3: The SFT vs. the magnetic field with different sizes of the quantum dots:(■) d= 20 nm,(●) d= 30 nm, (▲) d= 40 nm, and (◆) d= 60 nm for $T = 4$ K (a) and 10 K (b).

the previous subsection. Moreover, one notices that the SRT drops dramatically with the dot size. For a dot with $d = 60$ nm, the SRT is more than 6 orders of magnitude faster than the one with $d = 20$ nm. This is understood that for larger dots, more energy levels are engaged in the spin-flip scattering and hence sharply reduce the SRT.

D. Temperature dependence of the SRT

We plot the SRT as a function of the temperature in Fig. 4 for a QD with $d = 40$ nm under three different magnetic fields. From the figure one finds that the SRT gets smaller with the increase of the temperature. Moreover, the smaller the magnetic field is, the faster the SRT drops with the temperature.

These features can be understood as follows: With the increase of the temperature, the phonon number $\bar{n}_{\mathbf{q}\lambda}$ gets larger. This enhances the electron-phonon scattering and leads to the larger transition probability. Moreover, unlike the previous work[10] where the difference between zero temperature and finite temperatures is just the phonon Bose distribution, we stress that for high temperatures, the occupation to the high energy levels becomes important and it is inadequate to consider only the lowest several levels. For lower magnetic fields, the space between different energy levels is smaller. Therefore, more levels are included in the energy regime determined by f_i in Eq. (10) which leads to a faster response to the temperature. This feature is more pronounced in the low temperature regime. For high temperatures, as there are already many levels included in the energy space, adding a few more levels does not change the SRT significantly. Consequently the rates of the decrease of the SRT with the temperature become similar for different magnetic fields when $T > 16$ K.

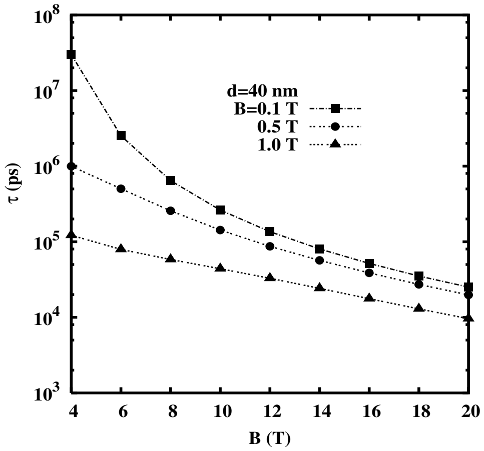

FIG. 4: The SRT *vs.* the temperature under different magnetic fields at $d = 40$ nm. Curve with ■: $B = 0.1$ T; Curve with ●: $B = 0.5$ T; and curve with ▲: $B = 1$ T.

E. Well width dependence of the SRT

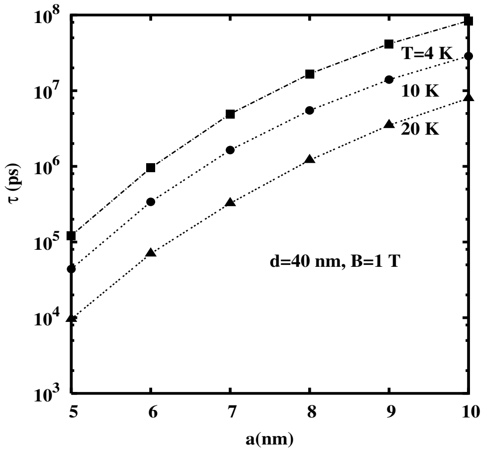

FIG. 5: The SRT *vs.* the width of the quantum well in different temperatures at B= 1 T. Curve with ■: $T = 4$ K; Curve with ●: $T = 10$ K; and Curve with ▲: $T = 20$ K.

As the QDs are confined in the quantum well, it is necessary to study the quantum well width dependence of the SRT as shown in Fig. 5 where τ is plotted as a function of the well width a for different temperatures at B=1 T. It is noted that the SRT increases with the well width a. This is due to the fact that the spin-orbit coupling H_{so} [Eq. (3)] is proportional to $1/a^2$. Smaller well width corresponds to larger spin-orbit coupling and therefore smaller SRT. We point out here that the well width in the present calculation is much smaller than the dot size d and only the lowest subband contributes to the SRT. For larger well width, more subbands are involved and hence there adds an opposite tendency for a shorter SRT with the increase of the well width.

IV. CONCLUSIONS

In conclusion, we have investigated the SRT in GaAs QDs by the exact diagonalization method with applied magnetic fields. After comparing the exact diagonalization method with the perturbation approach widely used in the literature, we find that the later is inadequate in accounting for the electron structure and the SRT in QDs. This is because that the energy splitting caused by the spin-orbit coupling is several times large than the Zeeman splitting used in the perturbation approach. Moreover, a lot more energy levels of H_0 are coupled by the spin-orbit coupling and therefore contribute to the lowest energy levels of the total QD Hamiltonian. We therefore reinvestigated the SRT from the exact diagonalization method to explore its dependence on the magnetic filed, the temperature and the size of the QD. We find the SRT decreases with the magnetic field, which is quite opposite to the bulk, the two- and one- dimensional cases. It also decreases with the diameter of the QD, but increases with the width of the quantum well on which the QD grows. For high temperature, the SRT becomes much faster due to the stronger electron-phonon scattering and the wider range of energy space the electron occupies. All our investigation suggests the importance of the exact calculation of the energy structure.

Acknowledgments

MWW is supported by the “100 Person Project” of Chinese Academy of Sciences and Natural Science Foundation of China under Grant No. 90303012. He would like to thank Dr. Marion Florescu for valuable discussion. The authors would like to acknowledge fruitful discussions with M. Q. Weng.

APPENDIX A: THE EXPRESSIONS OF $A^{(1)}$, $A^{(2)}$ AND $A^{(3)}$

$A^{(1)}$, $A^{(2)}$ and $A^{(3)}$ in Eq. (8) are given by

$$\begin{aligned} A^{(1)}_{n,l,n',l'} &= \alpha \int_0^\infty r^2 R_{n,l}(r) R_{n',l'}(r) dr \ , && \text{(A1)} \\ A^{(2)}_{n,l,n',l'} &= \frac{1}{\alpha} \int_0^\infty R_{n,l}(r) R_{n',l'}(r) dr \ , && \text{(A2)} \\ A^{(3)}_{n,l,n',l'} &= \frac{1}{\alpha} \int_0^\infty r R_{n,l}(r) \frac{\partial}{\partial r} R_{n',l'}(r) dr \ , && \text{(A3)} \end{aligned}$$

where $R_{n,l} = \sqrt{\frac{\alpha^2 n!}{\pi(n+|l|)!}}(\alpha r)^{|l|} \exp{(-\frac{(\alpha r)^2}{2})} L_n^{|l|}(\alpha^2 r^2)$ is the spatial part of the wave function Eq. (5). From the integration over the angular part, we get the relation $|l - l'| = 1$. Substituting this relation into Eqs. (A1)-(A3), after carrying out the integration we have

$$A^{(1)}_{n,l,n',l'} = \frac{1}{2\pi}(\sqrt{n+|l|+1}\delta_{n,n'} - \sqrt{n}\delta_{n',n-1}) \ , \qquad \text{(A4)}$$

$$A^{(2)}_{n,l,n',l'} = \begin{cases} \frac{1}{2\pi}\sqrt{\frac{n'!(n+|l|)!}{n!(n'+|l'|)!}}, & \text{if } n' > n \\ 0, & \text{otherwise} \end{cases} . \qquad \text{(A5)}$$

It is noted that due to the symmetry between {n, l} and $\{n', l'\}$, in above two equations we only give the results with $|l'| = |l| + 1$. Finally

$$A^{(3)}_{n,l,n',l'} = |l'| A^{(2)}_{n,l,n',l'} + A^{(1)}_{n,l,n',l'} - \begin{cases} \frac{\sqrt{n+|l|}}{\pi}, & \text{if } |l'| = |l| - 1 \text{ and } n' = n \\ \frac{|l'|}{\pi}\sqrt{\frac{n'!(n+|l|)!}{n!(n'+|l'|)!}}, & \text{if } |l'| = |l| + 1 \text{ and } n' \geqslant n \\ \frac{\sqrt{n}}{\pi}, & \text{if } |l'| = |l| + 1 \text{ and } n' = n - 1 \\ 0, & \text{otherwise} \end{cases} . \qquad \text{(A6)}$$

APPENDIX B: THE EXPRESSION OF $\Gamma_{i\to j}$

$$\Gamma_{i\to f} = \sum_{\lambda} \frac{1}{(2\pi)^2 v_\lambda} N_q \int_0^q dQ \frac{qQ}{q_z} \exp(-\frac{Q^2}{2\alpha^2}) G_{i,f}^2(\frac{Q^2}{(2\alpha)^2}, q_z) \int_0^{2\pi} d\theta |M_{q,\lambda}|^2 \tag{B1}$$

with $\mathbf{q} = (Q\cos\theta, Q\sin\theta, q_z)$ and $q = |\mathbf{q}| = \frac{|E_i - E_j|}{v_\lambda}$. Here $N_q = \bar{n}_q$ if $E_i > E_j$ or $\bar{n}_q + 1$ if $E_i < E_j$. $G_{i,f}$ in Eq. (B1) is

$$G_{i,f}(Q^2/(4a^2), q_z) = \sum_{n_1,l_1,n_2,l_2,\sigma} C^i_{n_1,l_1,\sigma} (C^f_{n_2,l_2,\sigma})^* \langle n_2, l_2| \exp[i(q_x x + q_y y)] |n_1, l_1\rangle \exp(\frac{Q^2}{2\alpha^2}) I(q_z) \ , \tag{B2}$$

in which

$$\begin{aligned} &\exp(\frac{Q^2}{2\alpha^2}) \langle n_2, l_2| \exp[i(q_x x + q_y y)] |n_1, l_1\rangle = \\ &\sqrt{\frac{n_1! n_2!}{(n_1 + |l_1|)!(n_2 + |l_2|)!}} e^{i(l_1 - l_2)(\frac{\pi}{2} + \theta)} (\mathrm{sgn}(l_1 - l_2) \frac{Q}{2\alpha})^{|l_1 - l_2|} \sum_{i=0}^{n_1} \sum_{j=0}^{n_2} \mathcal{C}^i_{n_1,|l_1|} \mathcal{C}^j_{n_2,|l_2|} n! L_n^{|l_1 - l_2|}(\frac{Q^2}{(2\alpha)^2}) \end{aligned} \tag{B3}$$

with sgn(x) denoting the sign function, $\mathcal{C}^m_{n,l} = \frac{(-1)^m}{m!}\binom{n+l}{n-m}$ and $n = i + j + \frac{|l_1| + |l_2| - |l_1 - l_2|}{2}$.

---

[*] Author to whom correspondence should be addressed; Electronic address: mwwu@ustc.edu.cn

[†] Mailing Address.

[1] *Semiconductor spintronics and quantum computation*, ed. by D. D. Awschalom, D. Loss, and N. Samarth (Springer-Verlag, Berlin, 2002).

[2] Manuel Valín-Rodríguez, Antonio Puente, and Llorenc Serra, Phys. Rev. B **66**, 235322 (2002).

[3] J. A. Gupta and D. D. Awschalom, Phys. Rev. B **59**, R10421(1999).

[4] A. V. Khaetskii and Yu. V. Nazarov, Physica E **6**, 470 (2000).

[5] B. Hackens, F.Delfosse, S. Faniel, C. Gustin, H. Boutry, X. Wallart, S. Bollaert, A. Cappy, and V. Bayot, Phys. Rev. B **66** 241305 (2002).

[6] Alexander V. Khaetskii and Yuli V. Nazarov, Phys. Rev. B **61**, 12639 (2000).

[7] Alexander V. Khaetskii and Yuli V. Nazarov, Phys. Rev. B **64**, 125316 (2001).

[8] O. Voskoboynikov, C. P. Lee, and O. Tretyak, Phys. Rev. B **63**, 165306 (2001).

[9] M. Governale, Phys. Rev. Lett., **89**, 206802 (2002).

[10] L. M. Woods, T. L. Reinecke, and Y. Lyanda-Geller, Phys. Rev. B **66**, 161318(R) (2002).

[11] M. I. D'yakonov and V. I. Perel', Zh. Eksp. Teor. Fiz. **60**, 1954 (1971), [Sov. Phys. JETP **38**, 1053 (1971)].

[12] W. Knap, C. Skierbiszewski, A. Zduniak, E. Litwin-Staszewska, D. Bertho, F. Kobbi, J. L. Robert, G. E. Pikus, F. G. Pikus, S. V. Iordanskii, V. Mosser, K. Zeketes, and Yu. B. Lyanda-Geller, Phys. Rev. B **53**, 3912 (1996).

[13] *Numerical Data and Functional Relationships in Science and Technology, Landolt-Börnstein, New Series*, edited by O. Madelung, M. Schultz, and H. Weiss (Springer-Verlag, Berlin, 1982), Vol. 17.

[14] M. W. Wu and C. Z. Ning, phys. stat. sol. (b) **222**, 523 (2000).

[15] M. Q. Weng and M. W. Wu, Phys. Rev. B **68**, 075312 (2003).

[16] J. L. Cheng, M. Q. Weng, and M. W. Wu, Solid State Commun. **128**, 365 (2003).